BEILSTEIN JOURNAL OF ORGANIC CHEMISTRY

Supporting Information

for

Phenanthridine–pyrene conjugates as fluorescent probes for DNA/RNA and an inactive mutant of dipeptidyl peptidase enzyme

Josipa Matić, Tana Tandarić, Marijana Radić Stojković, Filip Šupljika, Zrinka Karačić, Ana Tomašić Paić, Lucija Horvat, Robert Vianello and Lidija-Marija Tumir

Beilstein J. Org. Chem. **2023,** *19,* 550–565. doi:10.3762/bjoc.19.40

Additional experimental data

Content

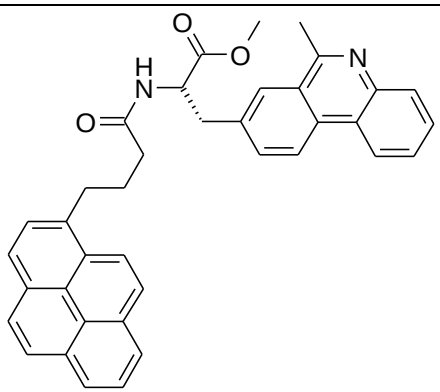

Phen-Py-1

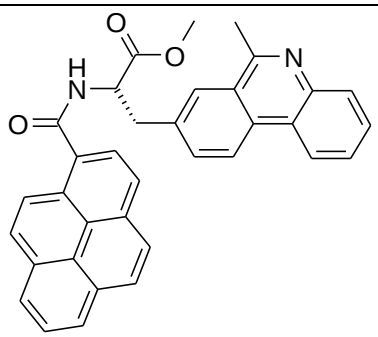

Phen-Py-2

Scheme 1. Structures of examined **Phen-Py-1** and **-2**.

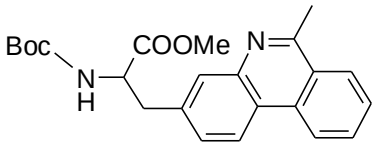

Phen-AA

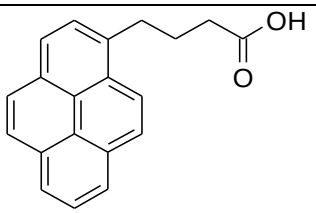

1-Pyrenebutyric acid (PBA)

Scheme 2. Structures of reference compounds.

1. Spectroscopic properties of Phen-Py-1 and -2

Studied compounds were moderately soluble in DMSO (up to $c = 1 \times 10^{-3}$ mol dm^{-3}). DMSO stock solutions of compounds were stable during few months. All measurements were recorded in Na-cacodylate buffer (I_c = 0.05mol dm^{-3}) both at pH 5.0 and pH 7.0. Volume ratio of DMSO was less than 1% in all measurements.

UV–vis spectra of examined compounds were recorded in Na-cacodylate buffer (I_c = 0.05mol dm^{-3}) both at pH 5 and pH 7. Further, spectra were recorded using immersion probe with 5 cm light path length, which allowed measurements at concentration range $5 \times 10^{-7} – 3 \times 10^{-6}$ mol dm^{-3} to avoid self-aggregation. Absorbancies of aqueous solutions of compounds **Phen-Py-1** and **2** were proportional to their concentrations up to concentrations $c = 3 \times 10^{-6}$ mol dm^{-3}. Thermal dependent UV–vis spectra

were recorded using quartz cuvettes (1 cm path). UV–vis spectra of aqueous solutions of examined compounds **1**–**2** showed minor irreversible changes upon heating that were attributed to precipitation. Absorption maxima and corresponding molar extinction coefficients (ε) were given in Table 1 and Figure S1.

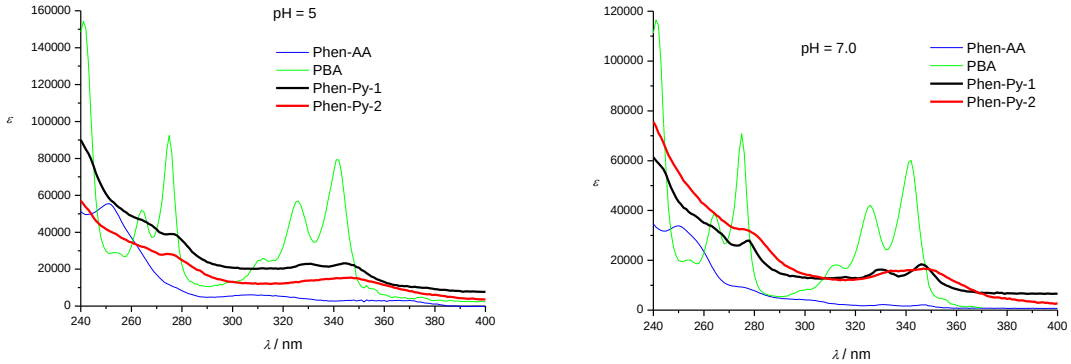

Figure S1. UV–vis spectra of **Phen-Py-1** and **2** and reference compounds **Phen-AA** and **PBA** at pH 5 and pH 7

Fluorescence emission of **Phen-Py-1** and **-2** measured at pH 5 and pH 7 (cacodylate buffer, I_c =0.05 mol dm^{-3}) was linearly dependent on the concentration up to 3 × 10^{-6} mol dm^{-3} (Figure S2).
Fluorescence intensity was decreased upon time and also upon temperature increase without reproducibility after cooling back. That was attributed to the temperature-induced unstacking of phenanthridine and pyrene but also aggregation/precipitation of the compounds.

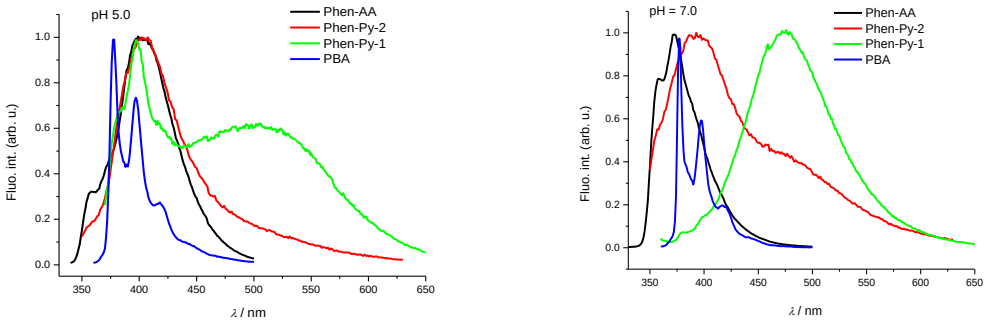

Figure S2. Normalized fluorescence emission spectra of **Phen-Py-1** (λ_{exc} = 350 nm), **Phen-Py-2** (λ_{exc} = 350 nm), reference Phen-AA (λ_{exc} = 250 nm) and reference PBA (λ_{exc} = 342 nm) compounds (sodium cacodylate buffer, I_c = 0.05 mol dm^{-3}, left: pH 5 right: pH 7)

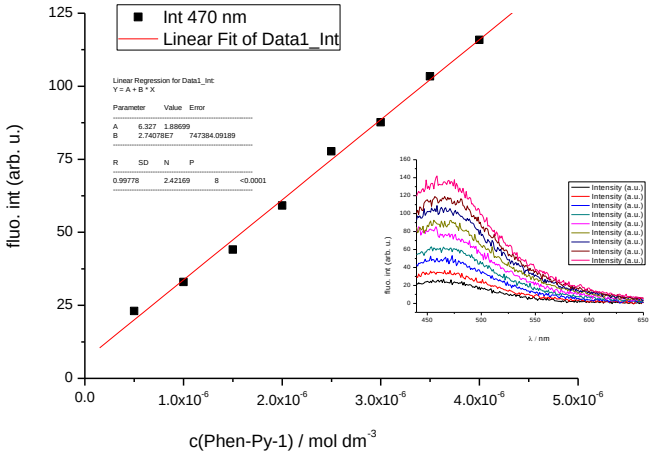

Figure S3 Linear dependence (—) of the fluorescence emission intensity of **Phen-Py-1** at 470 nm (■) Inset: Excimer emission spectra of **Phen-Py-1** (λ_{exc} = 350 nm, sodium cacodylate buffer, I_c = 0.05 mol dm^{-3}, pH 7)

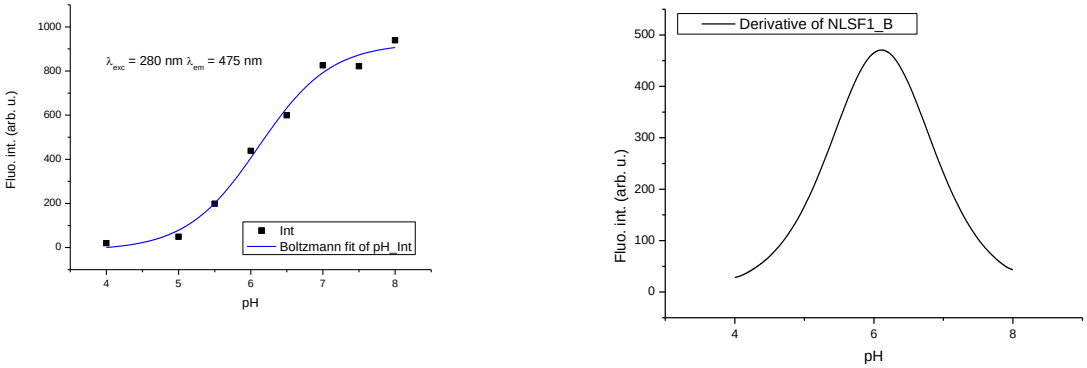

Figure S4. Left: Fluorescence emission spectra (λ_{exc} = 280 nm; λ_{em} = 475 nm)of **Phen-Py-1** (c = 2 × 10^{-6} mol dm^{-3}) at different pH values (Na-cacodylate, HCl, I_c = 0.05 mol dm^{-3} at 25 °C); Right: First derivation of fluorescence emmision at 475 nm in dependence of pH.

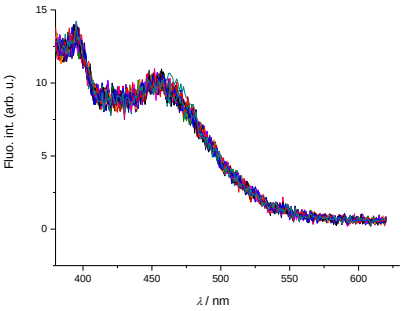

Figure S5. Fluorescence emission spectra of **Phen-Py-1** (c = 2 × 10^{-6} mol dm^{-3}) measured during 60 cycles every 2 minutes at 25 °C, λ_{exc} = 352 nm in methanol.

2. Study of interactions of Phen-Py-1 and -2 with ds-DNA and ds-RNA in aqueous media

2.1. Thermal melting experiments

Non-covalent binding of small molecules to ds-polynucleotides usually has a certain effect on the thermal stability of helices thus giving different T_m values (temperature of dissociation of double stranded helix into two single stranded polynucleotides)[1]. Difference between T_m value of free polynucleotide and complex with a small molecule (ΔT_m value) is an important factor in the characterisation of small molecule / *ds*-polynucleotide interactions. All thermal melting experiments were performed sodium cacodylate buffer, pH 7.0, I_c = 0.05 mol dm^{-3}.

At pH 7 **Phen-Py-1** and **Phen-Py-2** didn't thermally stabilize any *ds*-DNA/RNA (Table S1,Figure S6-S8).

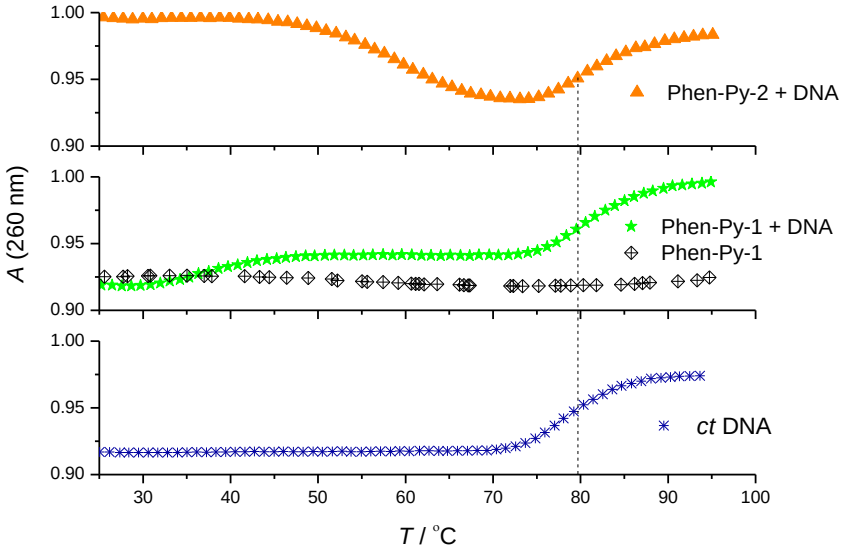

Figure S6. Melting curves of **Phen-Py-1** (c= 5 ×10^{-6} mol dm^{-3}) and *ct*-DNA upon addition of **Phen-Py-1** and **Phen-Py-2** (c(DNA)= 2 × 10^{-5} mol dm^{-3}; ratio r[compound] / [polynucleotide] = 0.3) at pH 7.0 (sodium cacodylate buffer, I_c = 0.05 mol dm^{-3}).

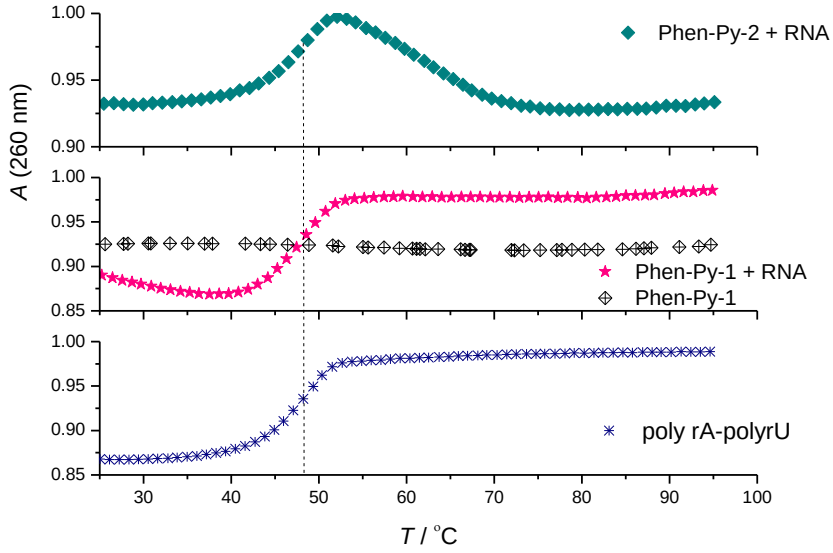

Figure S7. Melting curves of **Phen-Py-1** (c= 5 × 10^{-6} mol dm^{-3}) and poly rA-poly rU upon addition of **Phen-Py-1** and **Phen-Py-2** (c(RNA)= 2 × 10^{-5} mol dm^{-3}; ratio r[compound] / [polynucleotide] = 0.3) at pH 7.0 (sodium cacodylate buffer, I_c = 0.05 mol dm^{-3}).

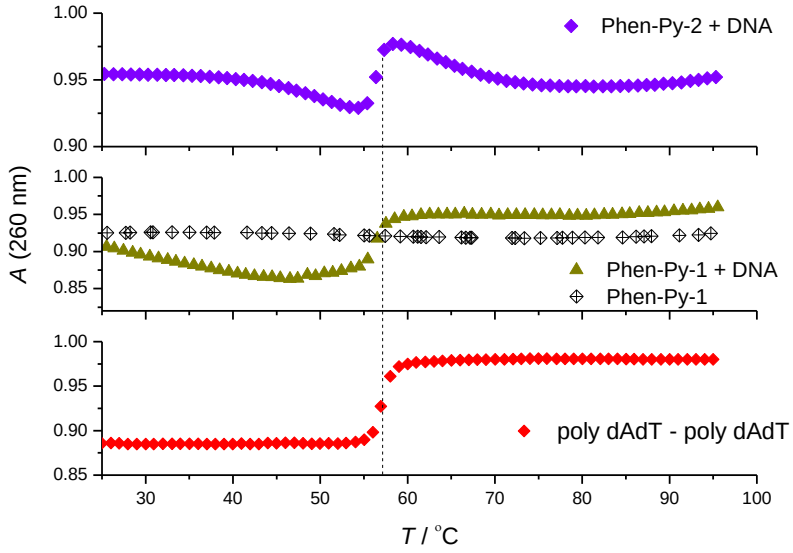

Figure S8. Melting curves of **Phen-Py-1** (c= 5 × 10^{-6} mol dm^{-3}) and poly dAdT – poly dAdT upon addition of **Phen-Py-1** and **Phen-Py-2** (c (DNA) = 2 × 10^{-5} mol dm^{-3}; ratio r[compound] / [polynucleotide] = 0.3) at pH 7.0 (sodium cacodylate buffer, I_c = 0.05 mol dm^{-3}).

Table S1. The [a]ΔT_m values (°C) of studied ds-polynucleotides upon addition of **Phen-Py-1** and **Phen-Py-2** (ratio r^b = 0.3) at pH 7.0 (buffer sodium cacodylate, I_c = 0.05 mol dm^{-3}), c(DNA / RNA) = 1–2 × 10^{-5} mol dm^{-3}.

	ΔT_m / °C		
Compound	***ct*-DNA**	**poly dAdT – poly dAdT**	**poly rA – poly rU**
Phen-Py-1	0	0	0
Phen-Py-2	precipitation	0	precipitation

[a] Error in ΔT_m : ± 0.5°C;

[b] r = [compound] / [polynucleotide];

[d] not determined due to precipitation

2.1. Spectrophotometric titrations

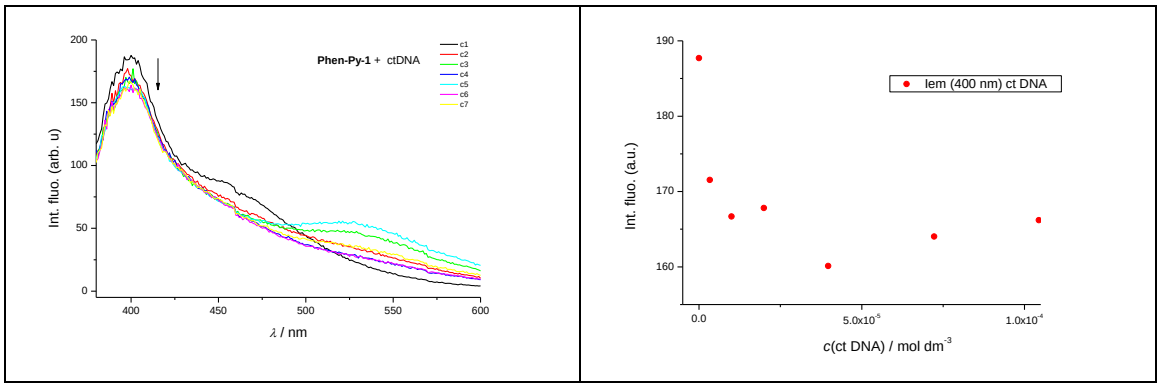

Figure S9. Left: Fluorimetric titration of **Phen-Py-1** with *ct*-DNA, λ_{exc} = 352 nm, c = 2 × 10^{-6} mol dm^{-3}, Right: Experimental (●) fluorescence intensities of **Phen-Py-1** at λ_{em} = 400 nm upon addition of *ct*-DNA (**pH 5.0**, Na cacodylate buffer, I_c = 0.05 mol dm^{-3}).

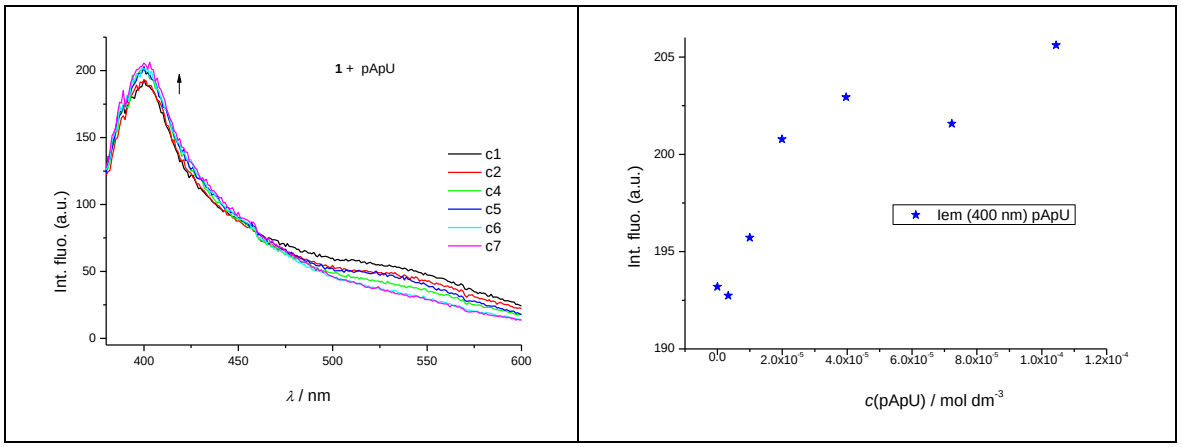

Figure S10. Left: Fluorimetric titration of **Phen-Py-1**, λ_{exc} = 352 nm, c = 2 × 10^{-6} mol dm^{-3} with poly rA-poly rU, Right: Experimental (●) fluorescence intensities of **Phen-Py-1** at λ_{em} = 400 nm upon addition of poly rA-poly rU (**pH 5.0**, Na cacodylate buffer, I_c = 0.05 mol dm^{-3}).

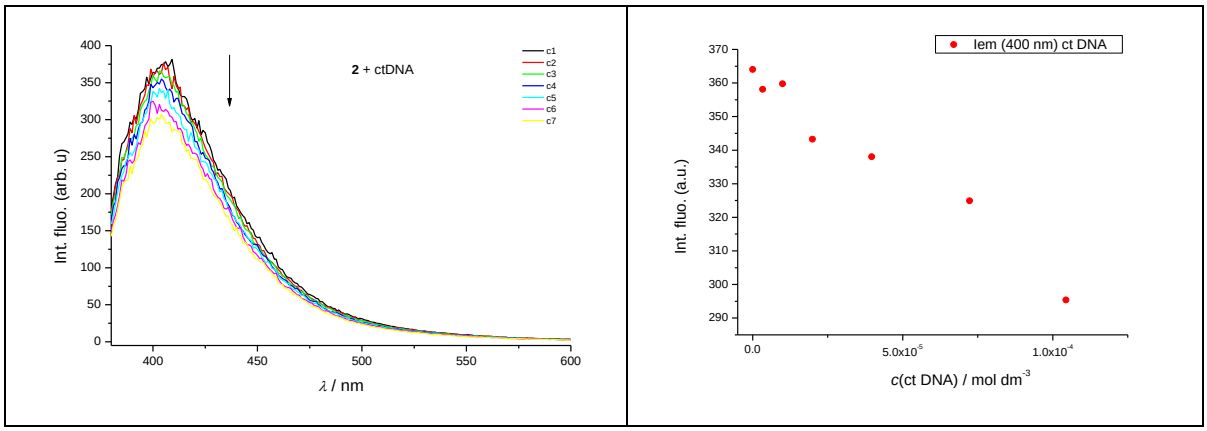

Figure S11. Left: Fluorimetric titration of **Phen-Py-2**, λ_{exc} = 352 nm, c = 2 × 10^{-6} mol dm^{-3} with *ct*-DNA, Right: Experimental (●) fluorescence intensities of **Phen-Py-2** at λ_{em} = 400 nm upon addition of *ct*-DNA (**pH 5.0**, Na cacodylate buffer, I_c = 0.05 mol dm^{-3}).

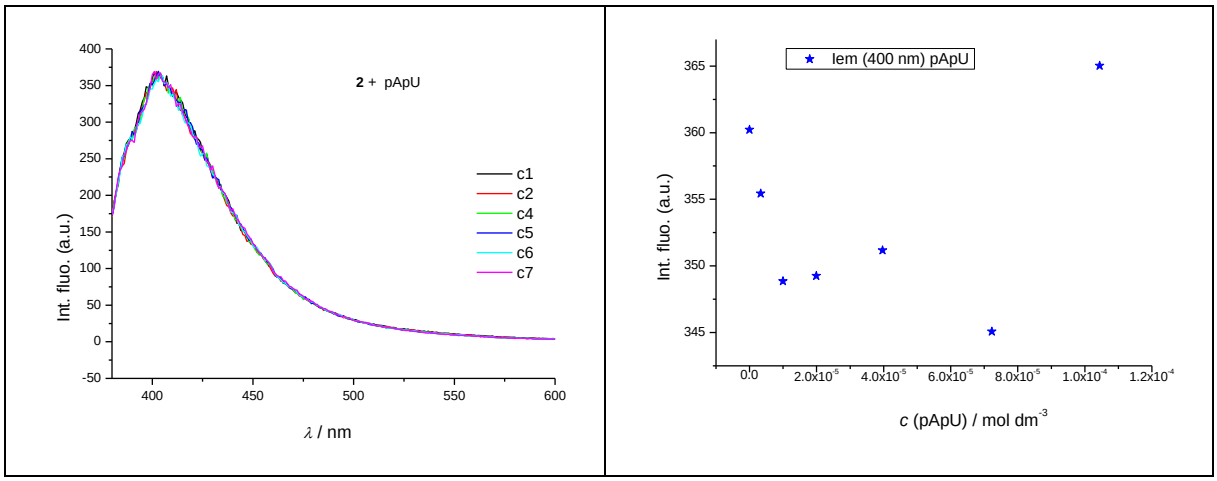

Figure S12. Left: Fluorimetric titration of **Phen-Py-2**, λ_{exc} = 352 nm, c = 2 × 10^{-6} mol dm^{-3} with poly rA-poly rU, Right: Experimental (●) fluorescence intensities of **Phen-Py-2** at λ_{em} = 400 nm upon addition of poly rA-poly rU (**pH 5.0**, Na cacodylate buffer, I_c = 0.05 mol dm^{-3}).

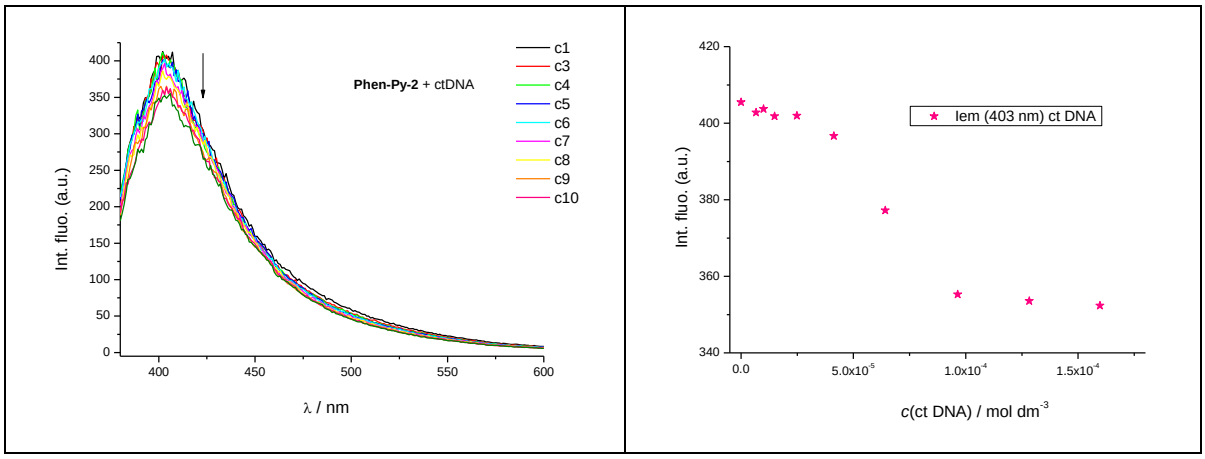

Figure S13. Left: Fluorimetric titration of **Phen-Py-2**, λ_{exc} = 352 nm, c = 2 × 10^{-6} mol dm^{-3} with *ct*-DNA, Right: Experimental (●) fluorescence intensities of **Phen-Py-2** at λ_{em} = 403 nm upon addition of *ct*-DNA (**pH 7.0**, Na cacodylate buffer, I_c = 0.05 mol dm^{-3}).

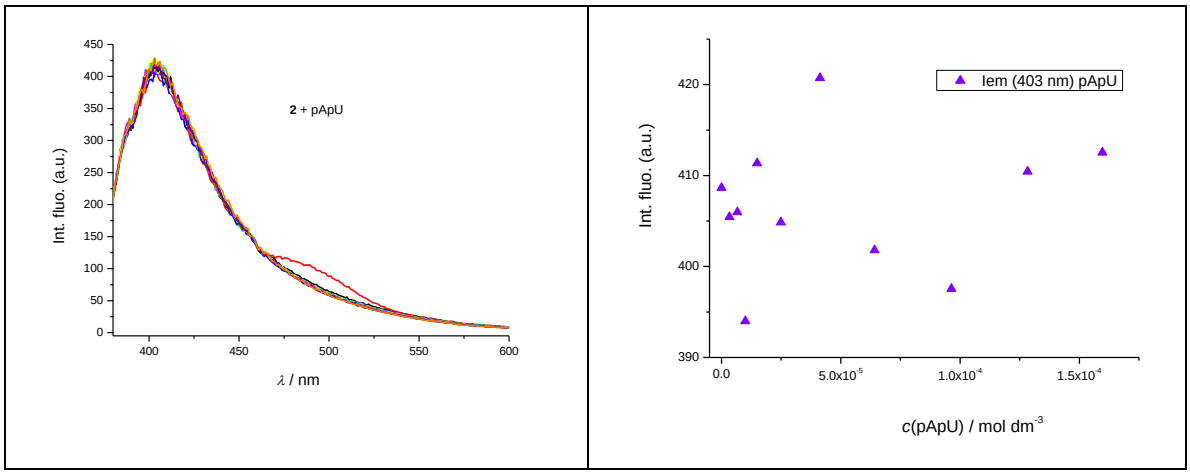

Figure S14. Left: Fluorimetric titration of **Phen-Py-2**, λ_{exc} = 352 nm, $c = 2 \times 10^{-6}$ mol dm^{-3} with poly rA-poly rU, Right: Experimental (●) fluorescence intensities of **Phen-Py-2** at λ_{em} = 400 nm upon addition of poly rA-poly rU (**pH 7.0**, Na cacodylate buffer, I_c = 0.05 mol dm^{-3}

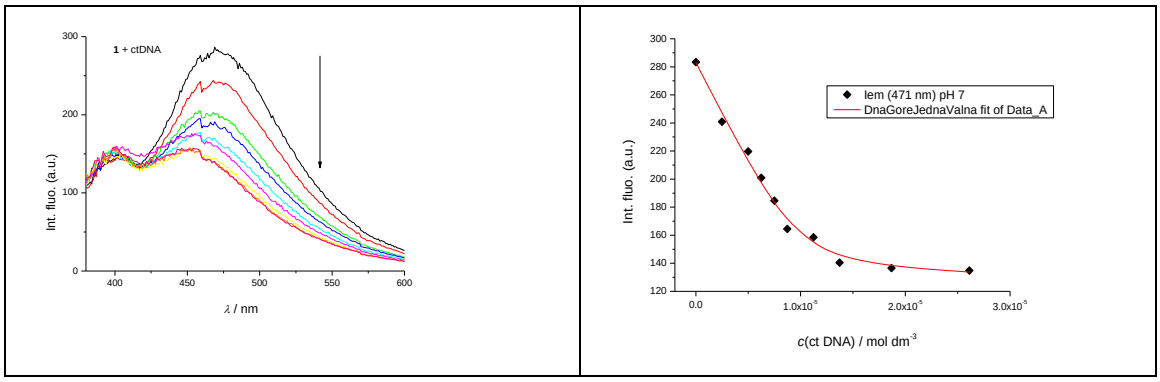

Figure S15. Left: Fluorimetric titration of **Phen-Py-1**, λ_{exc} = 352 nm, $c = 2 \times 10^{-6}$ mol dm^{-3} with *ct*-DNA, Right: Experimental (●) fluorescence intensities of **Phen-Py-1** at λ_{em} = 471 nm upon addition of *ct*-DNA (**pH 7.0**, Na cacodylate buffer, I_c = 0.05 mol dm^{-3}).

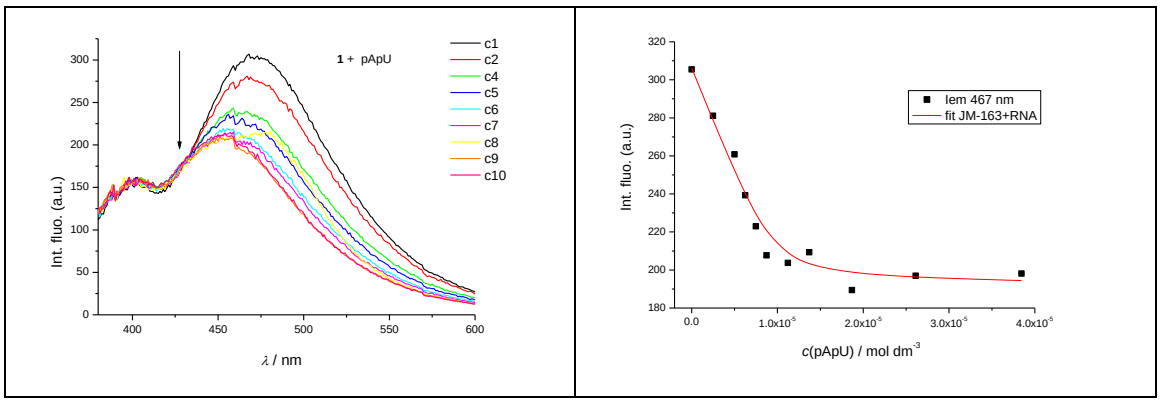

Figure S16. Left: Fluorimetric titration of **Phen-Py-1**, λ_{exc} = 352 nm, $c = 2 \times 10^{-6}$ mol dm^{-3} with poly rA-poly rU, Right: Experimental (●) fluorescence intensities of **Phen-Py-1** at λ_{em} = 467 nm upon addition of poly rA-poly rU (**pH 7.0**, Na cacodylate buffer, I_c = 0.05 mol dm^{-3}).

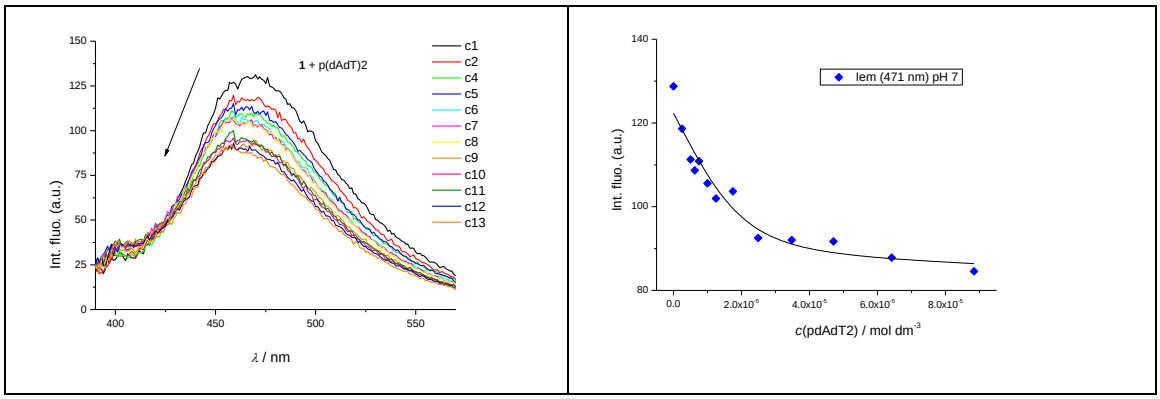

Figure S17. Left: Fluorimetric titration of **Phen-Py-1**, λ_{exc} = 352 nm, $c = 2 \times 10^{-6}$ mol dm^{-3} with poly dAdT - poly dAdT, Right: Experimental (●) fluorescence intensities of **Phen-Py-1** at λ_{em} = 471 nm upon addition of poly dAdT - poly dAdT (pH 7.0, Na cacodylate buffer, I_c = 0.05 mol dm^{-3}).

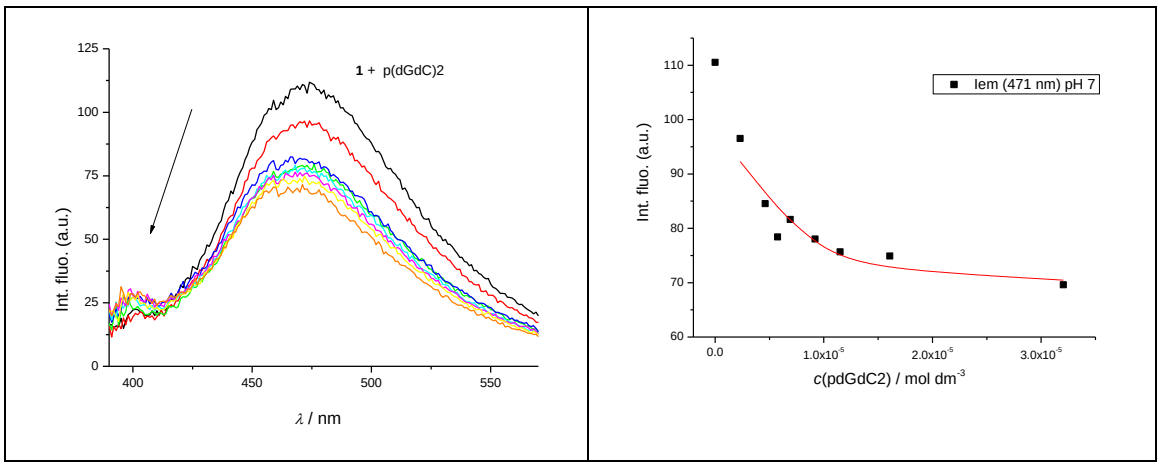

Figure S18. Left: Fluorimetric titration of **Phen-Py-1**, λ_{exc} = 352 nm, $c = 2 \times 10^{-6}$ mol dm^{-3} with poly dGdC - poly dGdC, Right: Experimental (●) fluorescence intensities of **Phen-Py-1** at λ_{em} = 471 nm upon addition of poly dGdC - poly dGdC (pH 7.0, Na cacodylate buffer, I_c = 0.05 mol dm^{-3}).

2.3. Circular dichroism (CD) experiments

CD spectroscopy was chosen to monitor conformational changes of polynucleotide secondary structure induced by small molecule binding[2]. Compounds **Phen-Py-1** and **Phen-Py-2** were built using chiral amino acid building blocks and consequently have intrinsic CD spectrum.

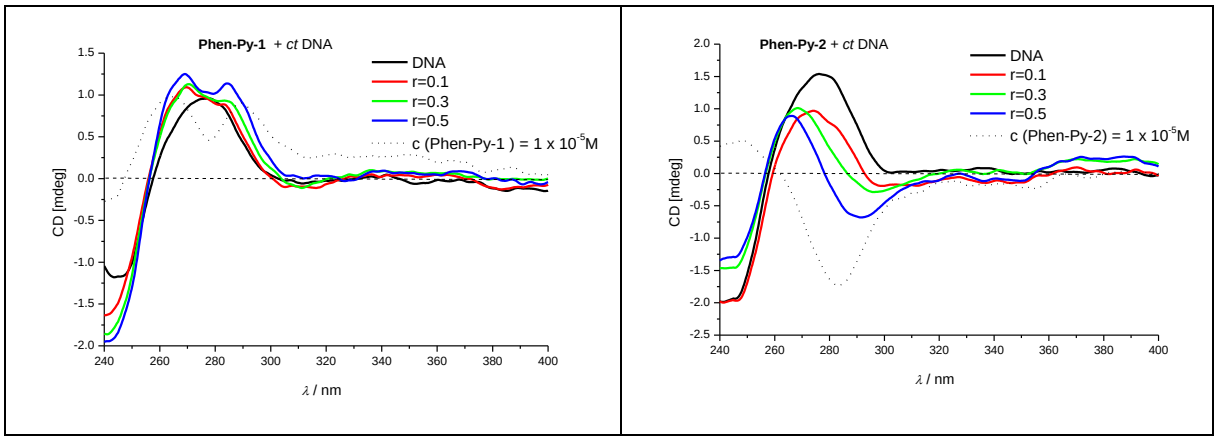

Figure S19. Changes in the CD spectrum of *ct*-DNA (c(DNA) = 2 × 10^{-5} mol dm^{-3}) upon addition of **Phen-Py-1** (left) and **Phen-Py-2** (right) at different molar ratios r = [compound] / [polynucleotide], pH 7.0, sodium cacodylate buffer, I_c = 0.05 mol dm^{-3}

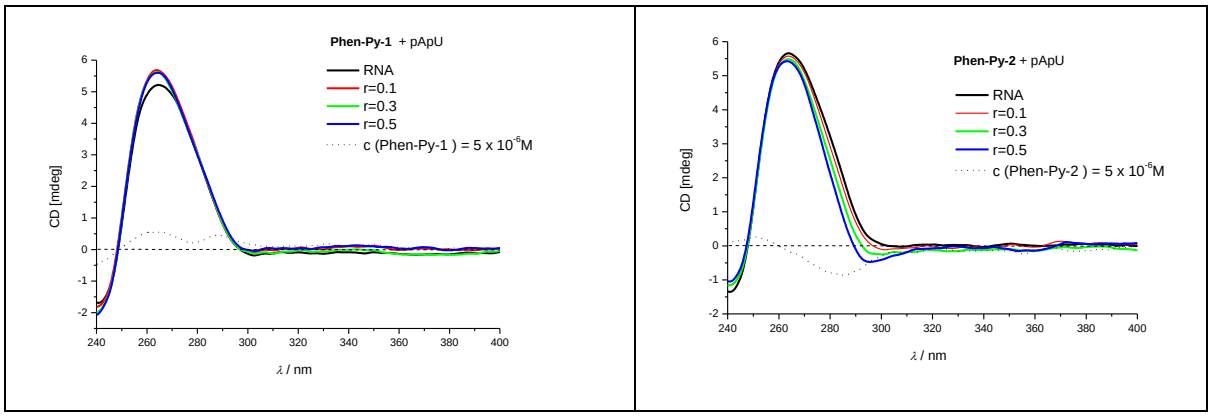

Figure S20. Changes in the CD spectrum of poly rA-poly rU upon addition of **Phen-Py-1** (c(RNA) =1 × 10^{-5} mol dm^{-3}) (left) and **Phen-Py-2;** (c(RNA) = 1 × 10^{-5} mol dm^{-3}) (right) at different molar ratios r = [compound] / [polynucleotide], pH 7.0, sodium cacodylate buffer, I_c = 0.05 mol dm^{-3}

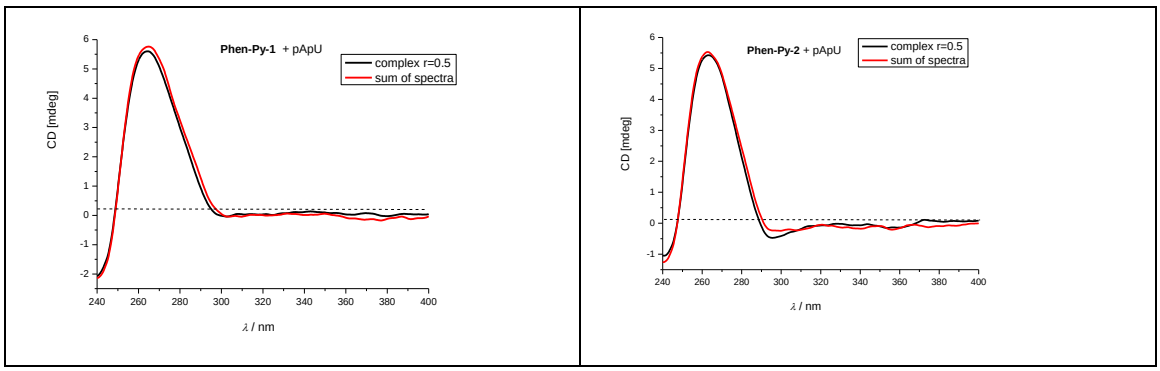

Figure S21. Comparation of spectra of RNA–dye complex (r= 0.5, —) and sum of poly rA-poly rU and dye spectra (—) of appropriate concentrations

3. NMR spectra of **Phen-Py-1** and **Phen-Py-2**

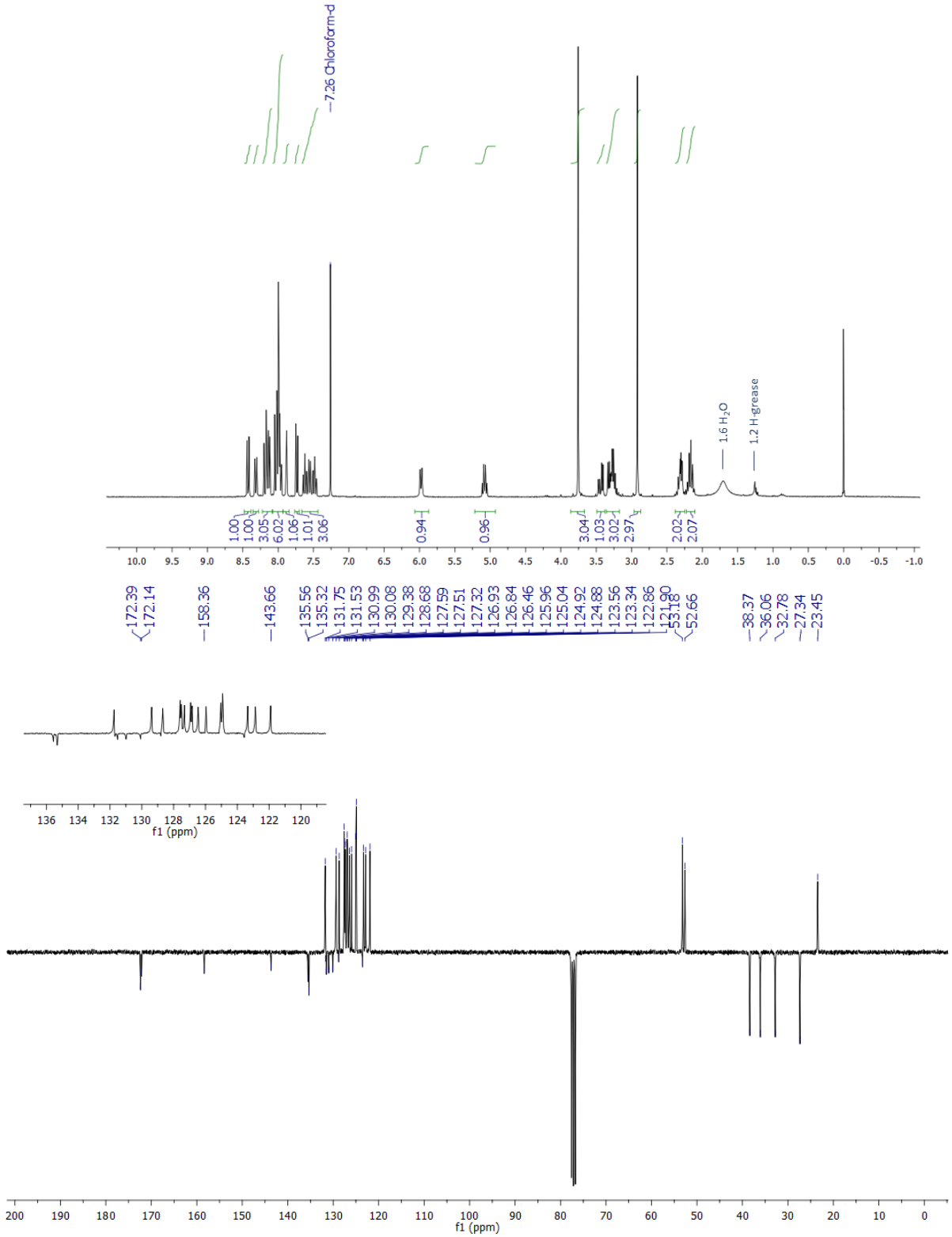

Figure S22. ^{1}H and ^{13}C NMR (APT) spectra of **Phen-Py-1**.

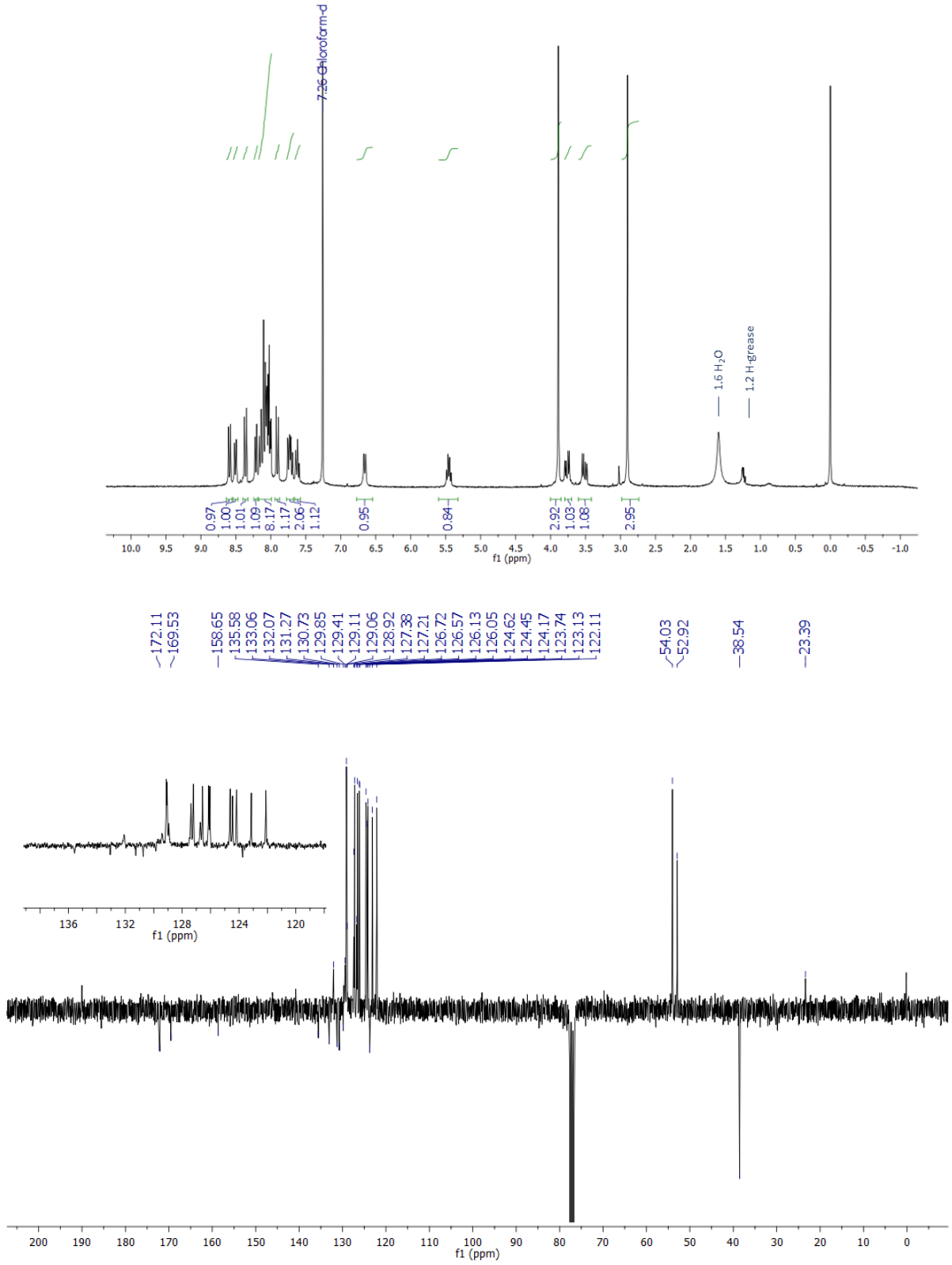

Figure S23. H and ^{13}C (APT) NMR spectra of **Phen-Py-2**.

4. Computational analysis

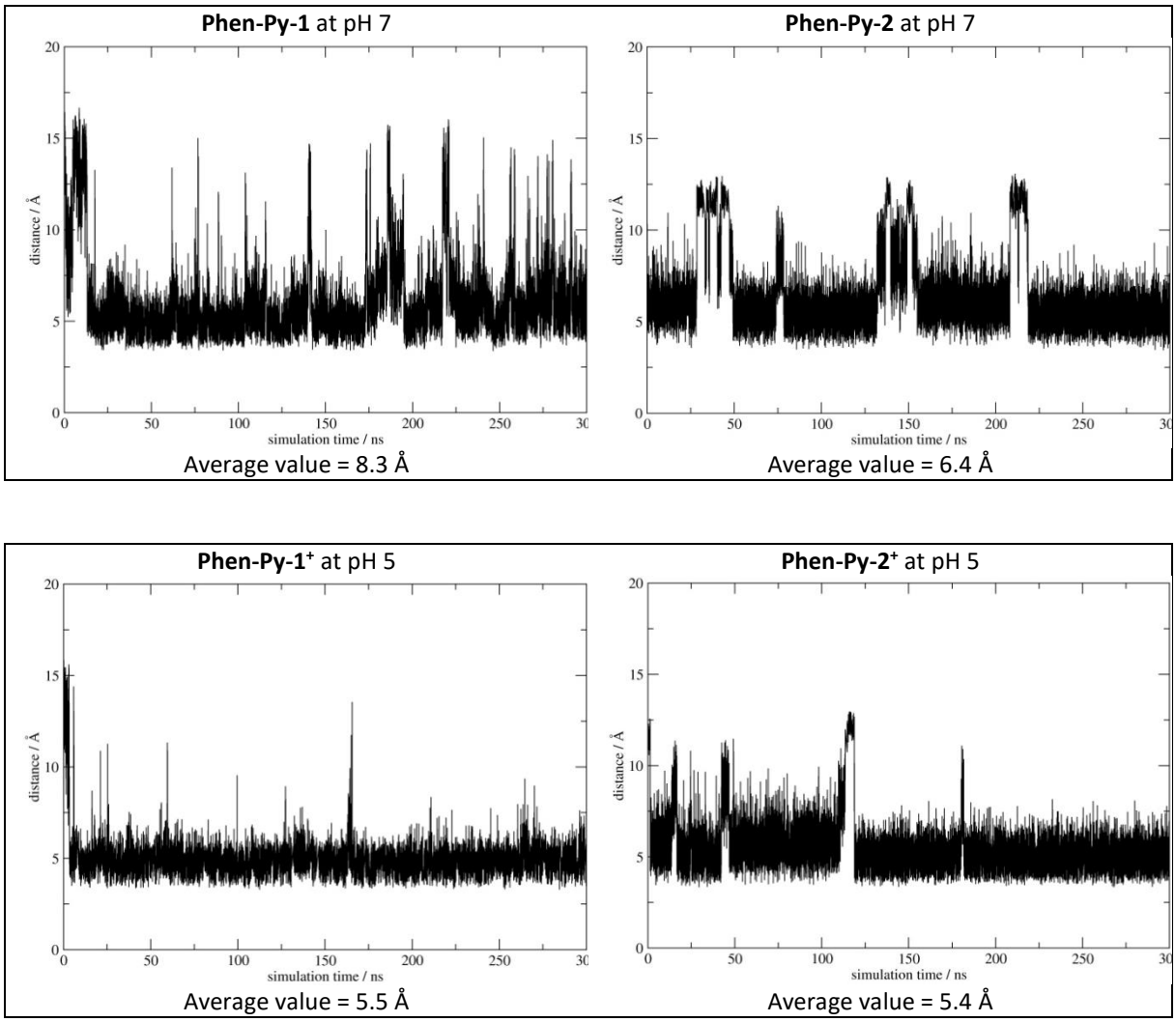

Figure S24. Evolution of distances between the centers of mass among pyrene and phenanthridine aromatic units during 300 ns of MD simulations in **Phen-Py-1** and **-2** conjugates under neutral (pH 7) and acidic (pH 5) conditions.

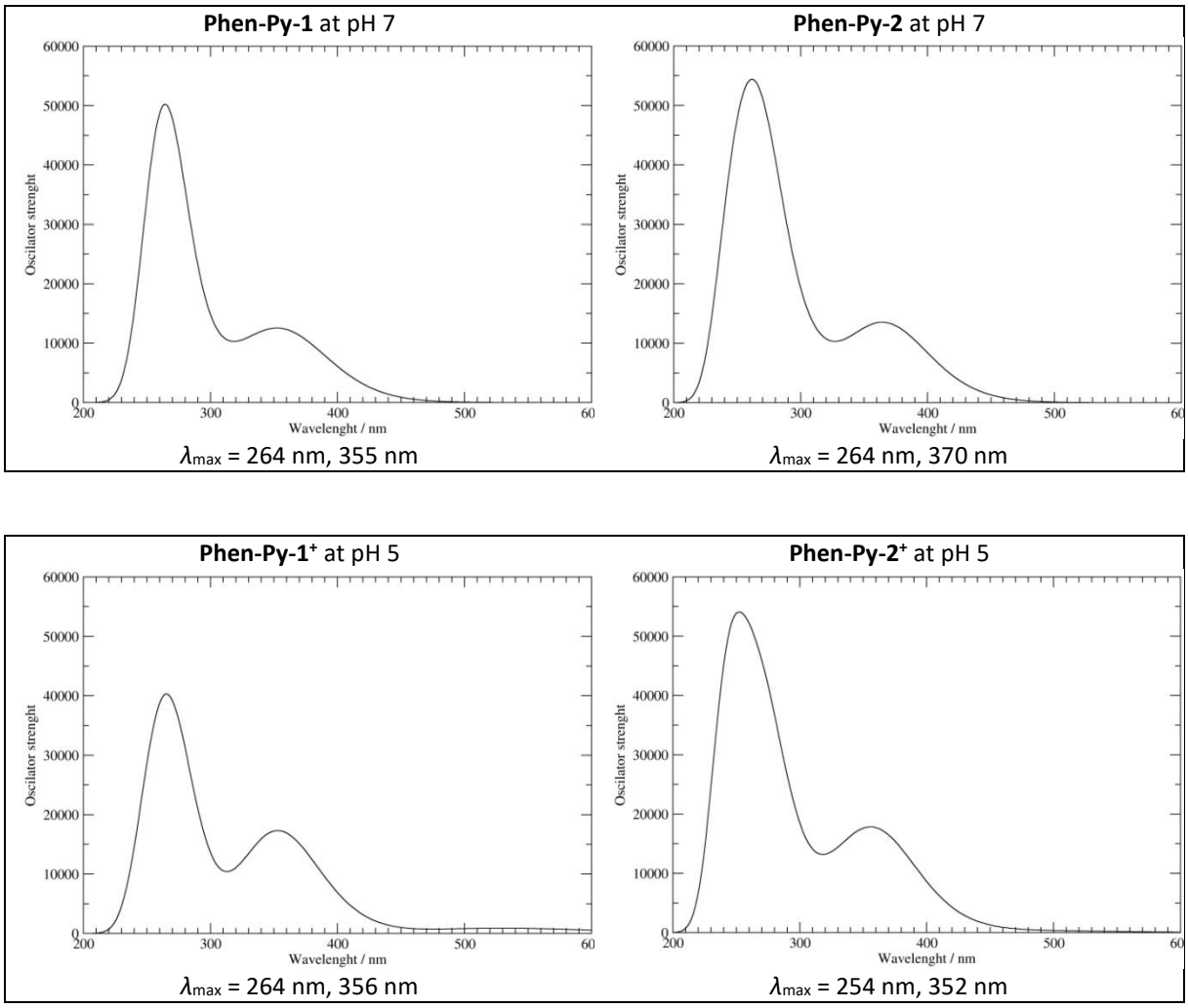

Figure S25. Calculated UV-Vis absorption spectra for **Phen-Py-1-2** conjugates under neutral (pH 7) and acidic (pH 5) conditions using the TD–DFT approach and the (IEF-PCM)/M06–2X/6–31+G(d) level of theory.

5. Confocal microscopy

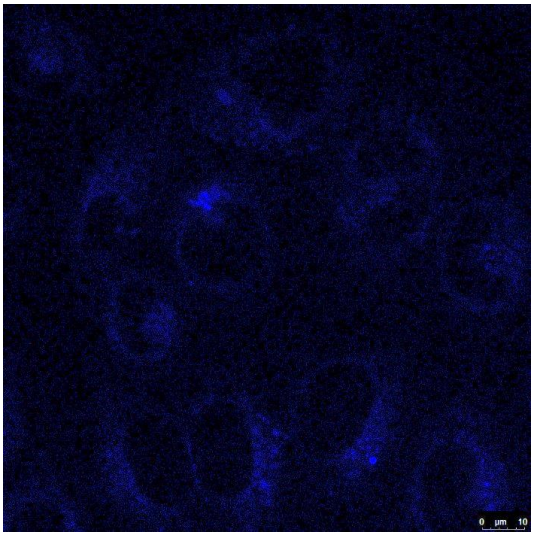

Figure S26. Live-cell image showing accumulation of **Phen-Py-1** dye (blue, 1 µM) in HeLa cells. Cells were treated with 1 µM of the compound and incubated for 60 min in 5% CO_2 at 37 °C. Scale bars, 10 mm. The **Phen-Py-1** dye excitation and emission profiles were previously measured and applied for confocal imaging.

Supporting Information References

[1] Mergny, J. L. and L. Lacroix (2003). "Analysis of thermal melting curves." Oligonucleotides **13**(6): 515-537.

[2] Rodger A., Norden B., In *Circular Dichroism and Linear Dichroism*; Oxford University Press: New York, 1997, Chapter 2.